

(corresponding to an infinite "off-diagonal" susceptibility), as has been suggested as a possibility in the analogous case of a two-dimensional Heisenberg ferromagnet.¹²

¹² See H. E. Stanley and T. A. Kaplan, Phys. Rev. Letters **17**, 913 (1966); J. Appl. Phys. **38**, 975 (1967); also G. S. Rushbrooke

^F Note added in proof. A discussion of the asymptotic behavior of the single-particle density matrix in restricted dimensionality has recently been presented by D. Jashow and M. E. Fisher, Phys. Rev. Letters **23**, 286 (1969).

and P. J. Wood, Proc. Phys. Soc. (London) **A68**, 1161 (1955); Mol. Phys. **1**, 257 (1958).

Surface Spin Waves for the Simple Cubic Antiferromagnet

T. WOLFRAM AND R. E. DE WAMES

Science Center, North American Rockwell Corporation, Thousand Oaks, California 91360

(Received 17 March 1969)

The surface spin-wave spectra of a simple cubic two-sublattice antiferromagnet is derived for a {100} surface as a function of the ratio ϵ of the surface exchange to the bulk exchange. The effects of changes in the surface anisotropy are also included. In general, a doubly-degenerate acoustical- or optical-type surface branch is found, depending upon the value of ϵ . For $-0.112 < \epsilon < 1.107$, an acoustic branch exists over the entire two-dimensional Brillouin zone. If $1.107 < \epsilon < 1.207$, then the branch is truncated at small values of the propagation vector k parallel to the surface. In the range $1.207 < \epsilon < 1.25$, no surface states exist for the nearest-neighbor-exchange model. When $1.25 < \epsilon < 1.854$, a truncated optical-type branch exists. A complete optical branch exists for $\epsilon \geq 1.854$. The $k=0$ surface-antiferromagnetic-resonance (SAFMR) mode lies very near the bulk AFMR mode for a wide range of surface perturbation parameters. The SAFMR mode is found to be of very long range when the anisotropy energy is small compared to the exchange energy. For simple cubic RbMnF₃, the SAFMR mode is estimated to have a range on the order of 200 μ .

I. INTRODUCTION

A NUMBER of studies of surface spin waves in magnetic systems have been reported recently.¹⁻⁷ The first study of the surface states of an antiferromagnet was reported by Mills and Saslow,⁴ who investigated the surface magnon spectrum of a free (unperturbed) {100} surface of a body-centered-cubic (bcc) two-sublattice Heisenberg antiferromagnet. They also estimated the effect of small perturbations in the surface parameters. A more recent study by De Wames and Wolfram⁷ treats in detail the effects of arbitrary changes in the surface exchange and surface anisotropy fields. In the latter study it was shown that both optical and acoustical spin-wave branches exist.

In this paper we report on a study of the surface spin-wave spectrum of the (100) surface of a two-sublattice simple cubic (sc) antiferromagnet as a function of the "in-plane" surface exchange and the surface anisotropy fields. There are many qualitative differ-

ences between this study and the study of the (100) surface of the bcc crystal because the latter surface contains spins of only one of the sublattices, while the sc (100) surface contains spins of both sublattices. This difference in the sublattice configurations leads to quite different results in the two cases for the energies of the surface antiferromagnetic resonance (SAFMR) corresponding to the propagation vector parallel to the surface, \mathbf{k} , being zero ($k=0$). In the bcc case the SAFMR lies lower than the bulk AFMR mode^{4,7} by a factor of approximately $\sqrt{2}$ whenever the anisotropy energy is much less than the exchange energy. This result is relatively insensitive to small perturbations in the surface exchange and anisotropy. The lowering of the SAFMR energy by the factor of $\sqrt{2}$ relative to the bulk mode is characteristic of a surface of a cubic two-sublattice antiferromagnet which has no exchange bonds parallel to the surface (in the nearest-neighbor-exchange approximation). In the case of the sc (100) surface, it is shown that SAFMR mode lies approximately at the sc bulk antiferromagnetic resonance energy under the same conditions as those described for the bcc case. This result is characteristic of surfaces of the cubic two-sublattice antiferromagnet in which the surface contains nearest-neighbor spins of both sublattices. For the sc antiferromagnet both optical and acoustical surface spin waves are found to exist. If the ratio ϵ of the surface exchange to the bulk exchange is less than

¹ J. R. Eshbach and R. W. Damon, J. Phys. Chem. Solids **19**, 308 (1961).

² B. N. Filippov, Fiz. Tverd. Tela **9**, 1339 (1967) [English transl. Soviet Phys.—Solid State **9**, 1048 (1967)].

³ R. F. Wallis, A. A. Maradudin, I. P. Ipatova, and A. A. Klochikhin, Solid State Commun. **5**, 89 (1966).

⁴ D. L. Mills and W. M. Saslow, Phys. Rev. **171**, 488 (1968).

⁵ C. F. Osborne, Phys. Letters **28A**, 364 (1968).

⁶ D. L. Mills, in *Localized Excitations in Solids*, edited by R. F. Wallis (Plenum Press, Inc., New York, 1968), p. 426.

⁷ R. E. De Wames and T. Wolfram (to be published).

1.107, a doubly degenerate acoustic surface spin-wave branch lower in energy than the corresponding bulk mode is found to exist for all values of k in the Brillouin zone. For $\epsilon > 1.107$, the acoustic branch exists for large k but is truncated at small k . As $\epsilon \rightarrow 1.207$, the acoustic branch degenerates to a single mode at the end of the Brillouin zone. For $1.207 < \epsilon < 1.25$, no surface wave solutions exist for the nearest-neighbor-exchange model. When $\epsilon \geq 1.25$, optical modes above the bulk spin-wave band appear. These optical branches are truncated at small k if $\epsilon < 1.854$, but are complete for $\epsilon \geq 1.854$.

In Sec. II, the surface spin-wave eigenvalue equation is derived using the random-phase approximation. A general solution is found for arbitrary changes in the surface anisotropy and exchange fields. In Sec. III, the general properties of the surface modes are discussed, and in Sec. IV some special results are derived. The surface spin-wave spectra are discussed in Sec. V. The two-sublattice Green's function is derived in Appendix A. The restrictions imposed on the surface mode solutions due to the boundary conditions on the Green's function are discussed in Appendices B and C. A brief discussion of the eigenvectors is presented in Appendix D.

II. THEORY

The Hamiltonian for the Heisenberg two-sublattice antiferromagnet with nearest-neighbor-exchange interaction is

$$\mathcal{H} = \sum_{i,\Delta} J(i, i+\Delta) \mathbf{S}_i^{(a)} \cdot \mathbf{S}_{i+\Delta}^{(b)} - \sum_i [g\mu_B H_0 + \omega_A(i)] S_{i,z}^{(a)} - \sum_j [g\mu_B H_0 - \omega_A(j)] S_{j,z}^{(b)}, \quad (1)$$

where $J(i, i+\Delta)$ is the exchange integral between nearest-neighbor spins located at \mathbf{R}_i and $\mathbf{R}_{i+\Delta}$, respectively. In this model, the nearest neighbors of a spin on sublattice a are on sublattice b . The anisotropy field is ω_A . The quantity H_0 is the external magnetic field, assumed to be directed along the z axis; μ_B is the Bohr magneton; g has its usual meaning; and $\mathbf{S}_i^{(\mu)}$ is the angular-momentum operator of the spin at \mathbf{R}_i on the μ th sublattice, whose α Cartesian component is $S_{i,\alpha}^{(\mu)}$. The sum over Δ is over the nearest-neighbor vectors. The sum over i is over the spins of the a sublattice, while the sum over j is over the b sublattice. Vectors \mathbf{R}_j and $\mathbf{R}_{i+\Delta}$ belong to the b sublattice, while \mathbf{R}_i and $\mathbf{R}_{j+\Delta}$ belong to the a sublattice. The coordinate system for the spin vectors is independent of the crystal coordinates. The external field here is referred to the spin coordinate system and is assumed to be along the direction of the sublattice magnetization.

We define the operators L_i and L_j by

$$\begin{aligned} L_i &= S_{i,x}^{(a)} + iS_{i,y}^{(a)}, \\ L_j &= S_{j,x}^{(b)} + iS_{j,y}^{(b)}. \end{aligned} \quad (2)$$

The equations of motion for these operators are determined by

$$i \frac{d}{dt} L_l(t) = [L_l(t), \mathcal{H}(t)], \quad l = i, j \quad (3)$$

where $[\dots]$ indicates the commutator. In the random-phase approximation, Eq. (3) yields

$$\begin{aligned} \omega L_i(\omega) &= - \sum_{\Delta} J(i, i+\Delta) \langle S_{i+\Delta, z}^{(b)} \rangle L_i(\omega) \\ &\quad + \langle S_{i,z}^{(a)} \rangle \sum_{\Delta} J(i, i+\Delta) L_{i+\Delta}(\omega) \\ &\quad + [\omega_H + \omega_A(i)] L_i(\omega). \end{aligned} \quad (4)$$

The brackets $\langle \dots \rangle$ indicate the thermal expectation value of the enclosed operator. The equation for $L_j(\omega)$ may be obtained from Eq. (4) by substituting j in place of i , interchanging a and b , and changing the sign of ω_A .

In Eq. (4) we have written $\omega_H(i) = g\mu_B H_0$, and also have introduced the Fourier component $L_l(\omega)$ defined by

$$L_l(t) = \int_{-\infty}^{+\infty} d\omega e^{-i\omega t} L_l(\omega), \quad l = i, j. \quad (5)$$

We consider a semi-infinite crystal extending from $x=0$ to $x=\infty$. Because of translational invariance in the y and z coordinates, the states of the system will be characterized by a two-dimensional propagation vector in the yz plane, \mathbf{k} . In addition, the quantities $J(i, i+\Delta)$, $\omega_A(i)$, and $\langle S_{i,z}^{(\mu)} \rangle$ will depend only upon the crystal x component of their arguments. In this paper we consider a model in which we retain only the surface perturbations. We take $J(i, i+\Delta)$ to be J_1 between spins on the surface and otherwise equal to the bulk value J . Similarly, we take $\omega_A(i)$ to be ω_{A1} on the surface and ω_A otherwise. We further restrict our considerations to zero temperature so that the thermal expectation value of the spin is uniform on each sublattice. We take $\langle S_{i,z}^{(a)} \rangle = -\langle S_{j,z}^{(b)} \rangle = \langle S \rangle$ at $T=0$.

We now consider the (100) surface of the sc structure and reduce our equation (4) to a one-dimensional matrix problem by introducing the functions $u_n^{(\mu)}(\omega)$ defined by

$$\begin{aligned} L_l(\omega) &= (2\pi d)^{-2} \int d\mathbf{k} e^{i\mathbf{k} \cdot \boldsymbol{\rho}_l} u_n^{(\mu)}(\mathbf{k}, \omega), \\ l &= i, j, \quad n = 1, 2, 3, \dots, \infty \end{aligned} \quad (6)$$

where $\mu = a$ for $l = i$ and b for $l = j$, and $\mathbf{R}_l = (\boldsymbol{\rho}_l, nd)$. The integral is over all two-dimensional \mathbf{k} belonging to the Brillouin zone of the sublattice whose spacing is d .

The $\mu = a$ component $u_n^{(a)}(\mathbf{k}, \omega)$ describes the x dependence of the spins of the a sublattice on the n th layer parallel to the (100) surface for a spin mode with propagation vector \mathbf{k} and energy ω . The $\mu = b$ component describes in a similar way the behavior of the b sub-

lattice spins. We obtain the supermatrix equation

$$(\bar{D} + \Delta\bar{D})U = 0, \tag{7}$$

where \bar{D} is the nearest-neighbor supermatrix of 2×2 matrices, and U is a column vector whose elements are two-component vectors

$$\bar{D} = \begin{pmatrix} D_0 & D_1 & 0 & 0 & 0 & \dots & 0 \\ D_1 & D_0 & D_1 & 0 & 0 & \dots & 0 \\ 0 & D_1 & D_0 & D_1 & 0 & \dots & 0 \\ 0 & 0 & D_1 & D_0 & D_1 & \dots & \\ \cdot & \cdot & \cdot & \cdot & \cdot & \dots & \\ \cdot & \cdot & \cdot & \cdot & \cdot & \dots & \\ \cdot & \cdot & \cdot & \cdot & \cdot & \dots & \end{pmatrix}, \tag{8}$$

$$U = \begin{pmatrix} \begin{matrix} u_1^{(a)}(k, \omega) \\ u_1^{(b)}(k, \omega) \end{matrix} \\ \begin{matrix} u_2^{(a)}(k, \omega) \\ u_2^{(b)}(k, \omega) \end{matrix} \\ \cdot \\ \cdot \\ \cdot \end{pmatrix}. \tag{9}$$

The matrices have elements defined by

$$D_0 = \begin{pmatrix} E - \omega_0 & -\omega_k \\ \omega_k & E + \omega_0 \end{pmatrix}, \tag{10}$$

$$D_1 = \begin{pmatrix} 0 & -1 \\ 1 & 0 \end{pmatrix}.$$

The perturbation supermatrix $\Delta\bar{D}$ has the first diagonal ΔD_0 as its only nonvanishing element:

$$\Delta D_0 = \begin{pmatrix} \Delta\omega_0 & +\Delta\omega_k \\ -\Delta\omega_k & -\Delta\omega_0 \end{pmatrix}. \tag{11}$$

The parameters occurring in Eqs. (10) and (11) are

$$\begin{aligned} E &= (\omega - \omega_H)/C, \\ \omega_0 &= 6 + \omega_A/C, \\ \omega_k &= 2(\cos \frac{1}{2} k_y d + \cos \frac{1}{2} k_x d), \\ C &= J\langle S \rangle, \\ \Delta\omega_0 &= 1 + 4(1 - \epsilon) - \Delta\omega_A, \\ \Delta\omega_A &= \omega_{A1} - \omega_A, \\ \epsilon &= J_1/J, \\ \Delta\omega_k &= \omega_k(1 - \epsilon). \end{aligned} \tag{12}$$

If we define the Green's function by $\bar{G} = \bar{D}^{-1}$, then the surface eigenstates are determined by the vanishing of the determinant of the matrix:

$$\det(\bar{I} + \bar{G}\Delta\bar{D}) = 0, \tag{13}$$

where \bar{I} is the unit supermatrix. Because of the simple form of $\Delta\bar{D}$, Eq. (13) reduces to the determinant of the upper 2×2 elements. The construction of the elements

of \bar{G} is described in Appendix A. We find that

$$\{\bar{G}\}_{nm} = \begin{pmatrix} \{\bar{G}\}_{nm}^{11} & \{\bar{G}\}_{nm}^{12} \\ \{\bar{G}\}_{nm}^{21} & \{\bar{G}\}_{nm}^{22} \end{pmatrix}, \tag{14}$$

where

$$\{\bar{G}\}_{nm}^{11} = \frac{1}{2} \left(\frac{\omega_0 + E}{\omega_0 - E} \right)^{1/2} [f_{nm}(\theta_1) - f_{nm}(\theta_2)]$$

and

$$\{\bar{G}\}_{nm}^{21} = \frac{1}{2} [f_{nm}(\theta_1) + f_{nm}(\theta_2)],$$

$$\{\bar{G}\}_{nm}^{22} = - \left(\frac{\omega_0 - E}{\omega_0 + E} \right) \{\bar{G}\}_{nm}^{11}, \tag{15}$$

$$\{\bar{G}\}_{nm}^{12} = -\{\bar{G}\}_{nm}^{21}.$$

The functions $f_{nm}(\theta_\beta)$ are given by

$$f_{nm}(\theta_\beta) = (2i \sin \theta_\beta)^{-1} (e^{i(n+m)\theta_\beta} - e^{i|n-m|\theta_\beta}) \tag{16}$$

and

$$-2 \cos \theta_\beta = \omega_k \pm (\omega_0^2 - E^2)^{1/2}. \tag{17}$$

In Eq. (17) the plus sign goes with $\beta = 1$, while the minus sign goes with $\beta = 2$. After some straightforward but tedious algebra, we obtain from Eqs. (13)–(17) the surface spin-wave spectrum:

$$E_k^2 = \omega_0^2 - \omega_k^2/x^2 - 4/(1-x^2), \tag{18}$$

where x is a root of the cubic equation

$$\begin{aligned} \Delta\omega_0\omega_0 x^3 - [1 - (\Delta\omega_k)\omega_k + (\Delta\omega_k)^2 - (\Delta\omega_0)^2]x^2 \\ - [(\Delta\omega_0)\omega_0 + (\Delta\omega_k)^2 - (\Delta\omega_0)^2 - 1]x \\ - (\Delta\omega_k)\omega_k = 0. \end{aligned} \tag{19}$$

Caution must be exercised when using Eqs. (18) and (19). The variable x is defined as

$$x = -i \cot \frac{1}{2}(\theta_1 + \theta_2). \tag{20}$$

We see from the form of the Green's function, Eq. (15), that both θ_1 and θ_2 must have positive imaginary parts. Consequently, only those values of x which correspond to both θ_1 and θ_2 lying in the upper-half complex plane are physically acceptable solutions of the surface-mode problem. The values of x derived from Eq. (19) which do not satisfy this criterion are not acceptable solutions. This point is discussed in detail in Appendix B.

III. GENERAL PROPERTIES OF SURFACE MODES

In this section we describe the general features of the surface spin-wave spectrum as a function of the various parameters. First we consider the spectrum of the bulk. In Fig. 1 we indicate by the shaded area the bulk continuum of spin-wave states as a function of the propagation vector parallel to the surface. The spectrum is given by

$$E^2 = (6 + \omega_A)^2 - (2 \cos \frac{1}{2} k_x d + \omega_k)^2. \tag{21}$$

For a fixed value of ω_k the range of E^2 is obtained by varying $\frac{1}{2} k_x d$ in Eq. (21) between zero and π . We shall

refer to the lower boundary of the shaded region, obtained by setting $\frac{1}{2}k_x d = 0$, as the bottom of the continuum. The top of the continuum is the maximum value of E^2 for a given ω_k . From Eq. (21) it follows that the top of the continuum is equal to $(6 + \omega_A)^2$ for $\omega_k \leq 2$. When $\omega_k \geq 2$, the upper boundary is given by Eq. (21) with $\frac{1}{2}k_x d = \pi$.

In general, surface eigenstates cannot exist within the bulk continuum of states. An excitation corresponding to a point (E^0, ω_k^0) in the continuum which is localized near the surface would decay rapidly into non-local bulk-type states. The lifetime of such an excitation would depend inversely upon the density of continuum states at (E^0, ω_k^0) . The various types of surface spin-wave branches which can occur are illustrated schematically in Fig. 1 for $\Delta\omega = 0$ and $\omega_A \ll \omega_0$. All of the spin-wave states are doubly-degenerate (in the variable E^2), corresponding to the two possible senses of spin precession. The surface modes change their nature at critical values of ϵ given by $\epsilon_a \approx -0.112$, $\epsilon_b \approx 1.107$, $\epsilon_c \approx 1.207$, $\epsilon_d \approx 1.25$, and $\epsilon_e \approx 1.854$. The curve labeled *A1* is a nontruncated acoustic-type branch which exists for the approximate range $\epsilon_a \leq \epsilon \leq \epsilon_b$. (The spin arrangement is unstable for $\epsilon < \epsilon_a$.) When $\epsilon_b < \epsilon < \epsilon_c$, one finds an acoustic branch which is truncated at small k (small values of $4 - \omega_k$). As ϵ increases, the point of truncation moves to larger k . Such a surface spin-wave branch is illustrated in Fig. 1 by the curve *A2*, which exists only for $\omega_k \geq \Omega_{AC}$. As $\epsilon \rightarrow \epsilon_c$, the *A2* branch degenerates into a single isolated mode at *E2*. In the range $\epsilon_c \leq \epsilon < \epsilon_d$, there are no surface spin waves. At $\epsilon = \epsilon_d$, a single isolated optical-type surface spin-wave mode appears at *E3*. As ϵ increases from ϵ_d , branches similar to those labeled *O2* and *O3* occur which are truncated at Ω_{OC} . Finally, for $\epsilon > \epsilon_e$ one finds a nontruncated optical branch similar to the curve labeled *O1*. It is also possible to obtain a segment of an *A2* branch. In Fig. 2, we illustrate such an example by the *A3* curve. In this example, $\epsilon > \epsilon_c$, so that the *A2* branch does not exist. By lowering the surface anisotropy field sufficiently, the segment *A3* is pushed off below the bottom of the continuum. Similarly, truncation of the *A1* curves can result at small k is the surface anisotropy is increased.

The critical values of ϵ mentioned above are easily obtained when $\omega_A = \Delta\omega_A = 0$. They depend only very weakly upon ω_A and $\Delta\omega_A$ when these parameters are small compared to the exchange energy. The critical values of ϵ are derived in the following sections.

IV. SPECIAL CASES

In this section we discuss the behavior of the surface spin-wave branches at special values of k , and also for special values of ϵ .

A. $k \approx 0$ ($\omega_k \approx 4$)

We consider first the dependence of the SAFMR on the value of ϵ . First, we assume that $\omega_A = \Delta\omega_A = 0$. It is

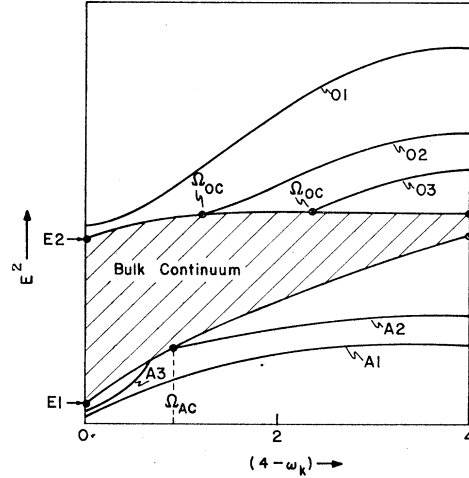


FIG. 1. Schematic illustration of the various possible acoustical and optical surface spin-wave branches. All branches are doubly-degenerate. The points indicated are $E1 = 12\omega_A + \omega_A^2$, $E2 = (6 + \omega_A)^2 - 4$, and $E3 = (6 + \omega_A)^2$.

easily established by direct substitution that at $k=0$ ($\omega_k=4$) the roots of the cubic equation (19) are

$$x = \pm\sqrt{\frac{2}{3}} \quad \text{and} \quad -4(1-\epsilon)/(5-4\epsilon). \quad (22)$$

In Appendix B it is shown that only negative values of x can lead to physical solutions. The root $x = -\sqrt{\frac{2}{3}}$ corresponds to the *A1* acoustic branch and yields $E^2=0$ (independent of the value of ϵ) for $\omega_A=0$, according to Eq. (18). One may also calculate x for ω_A and $\Delta\omega_A \ll \omega_0$. To first order we find that

$$x = -\sqrt{\frac{2}{3}} + O(\omega_A/\omega_0). \quad (23)$$

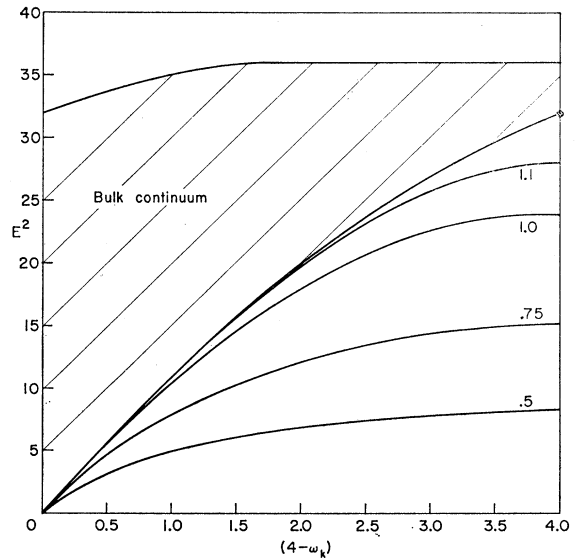


FIG. 2. Acoustic-type surface spin-wave branches as a function of ϵ for $\omega_A = \Delta\omega_A = 0$. Curves for $\epsilon > 1.107$ are truncated at the point at which they intersect the bottom of the bulk continuum.

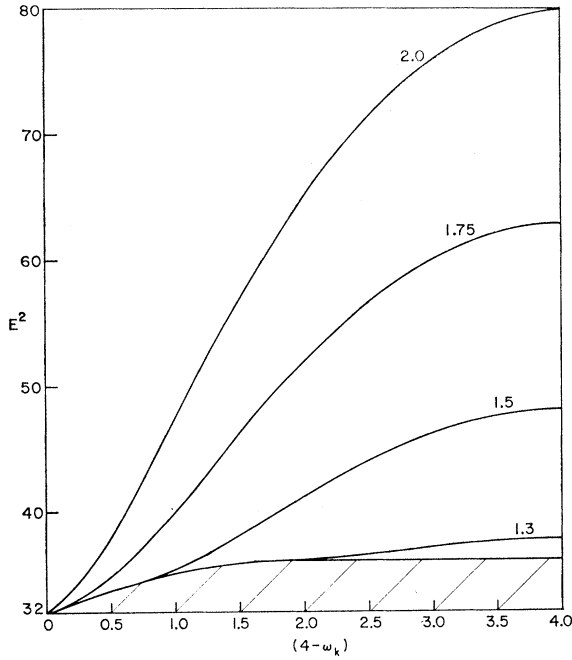


FIG. 3. Optical-type surface spin-wave branches as a function of ϵ for $\omega_A = \Delta\omega_A = 0$. Curves for $\epsilon < 1.854$ are truncated at the point at which they intersect the top of the bulk continuum.

Then, from Eq. (18), we find that

$$E_{(k=0)}^2 = 12\omega_A + O((\omega_A/\omega_0)^2).$$

Since the bulk AFMR mode has $E^2 = 12\omega_A$, we conclude that the SAFMR mode energy lies near that of the bulk AFMR for reasonable surface perturbations. This contrasts with the result in the bcc, in which the SAFMR mode lies lower than the bulk AFMR mode by a factor of $\sqrt{2}$.

The above analysis applies only to those spin-wave acoustic branches which exist for small k . When $\epsilon > \epsilon_b$ and $\omega_A \neq 0$, the surface acoustic branch does not exist at $k=0$. The value of $\epsilon_b = 1.107$ is obtained by studying the behavior of the $-\sqrt{2/3}$ root for small k ; this is described in Appendix C.

Next we consider the last root of Eq. (22), x_3 . For $\epsilon_a < \epsilon < 0$ (ferromagnetic surface exchange), x_3 corresponds to a latent instability of the system. As ϵ decreases to $\epsilon = -(\frac{3}{4}\sqrt{2/3} - \frac{1}{2}) = \epsilon_a$, it can be seen that $x_3 \rightarrow -\sqrt{2/3}$. For values of $\epsilon < \epsilon_a$, the spin arrangement is unstable at and near the surface. For $\epsilon > 0$, x_3 corresponds to a latent optical mode. As ϵ increases towards $(\frac{3}{2} + \frac{1}{4}\sqrt{2}) = \epsilon_c$, the cutoff Ω_{OC} of the optical mode $O2$ approaches $k=0$ (or $\omega_k=4$), and, finally for $\epsilon \geq \epsilon_c$, the $O1$ nontruncated optical branches exist.

B. $\epsilon = 1$

If $\epsilon = 1$, then $\Delta\omega_k = 0$ and the roots of the cubic are independent of ω_k . For $\Delta\omega_A = 0$ we obtain an $A1$ acoustic

branch from the root

$$x = -[(\omega_0 - 2)/\omega_0]^{1/2}, \quad (24)$$

with the spectrum

$$E^2 = \omega_0^2 - 2\omega_0 - \omega_k^2\omega_0/(\omega_0 - 2), \quad \epsilon = 1, \quad \Delta\omega_A = 0. \quad (25)$$

The other two roots for $\epsilon = 1$ do not correspond to physical solutions.

C. $\epsilon = \epsilon_a$ or ϵ_c

We encounter another special case when $\epsilon = 5/4 = \epsilon_a$ since, in this case, the increase in the surface exchange is just equal to the loss due to the missing neighbors. For $\omega_A = \Delta\omega_A = 0$, the coefficient of the cubic term of Eq. (19) vanishes. Examination of the two roots of the quadratic equations shows that neither is an acceptable root, except at the isolated point $E = 0$ and $\omega_k = 4$. This mode is an undamped bulk mode and does not properly belong to the surface wave spectrum. If $\omega_A \neq 0$, then there are no solutions for $\epsilon = 5/4$. If, however, $\epsilon \rightarrow 5/4$ from above for $\omega_k = 0$, then we obtain an isolated solution at $E^2 = \omega_0^2$ with $x \rightarrow -\infty$. This mode corresponds to the first appearance of an optical mode of the $O3$ type. In this case the $O3$ branch has degenerated into an isolated point.

When $\epsilon \rightarrow \frac{1}{2}(1 + \sqrt{2}) = \epsilon_c \approx 1.207$, the coefficient of the linear term in Eq. (19) vanishes. A similar analysis shows that if $\omega_k = 0$ and $\epsilon \rightarrow \epsilon_c$ from below, then an isolated mode at $E^2 = \omega_0^2 - 4$ exists for $x \rightarrow 0$ from below. This mode is an $A2$ acoustical branch which has degenerated into a single point.

No solutions are obtained when $\epsilon \rightarrow 5/4$ from below or $\epsilon \rightarrow \frac{1}{2}(1 + \sqrt{2})$ from above.

V. RESULTS AND DISCUSSION

The surface spin-wave spectra for various values of ϵ with $\omega_A = \Delta\omega_A = 0$ are shown in Figs. 2 and 3. The acoustical branches are shown in Fig. 2 and the optical branches in Fig. 3. The dependence of the SAFMR mode on ϵ is illustrated in Fig. 4 for several values of ω_A . The SAFMR mode lies very near the bulk AFMR mode and, for small ω_A , is very insensitive to the value

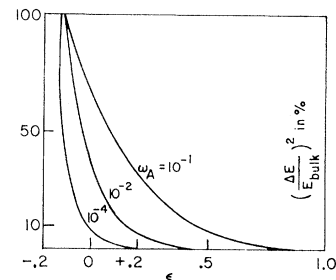


FIG. 4. Dependence of the SAFMR mode on ϵ for various values of ω_A . The parameter ΔE is the difference in energy between the SAFMR mode and the bulk AFMR energy E_{bulk} . The ordinate is the square of the ratio ΔE to E_{bulk} (in %).

of the surface exchange energy until it approaches zero. For negative ϵ (ferromagnetic exchange) the mode approaches zero frequency corresponding to the instability of the ground state to spin rearrangement. In Fig. 5 we show the dependence of the surface mode energy on ϵ for small k .

It is evident from Figs. 2 and 3 that the nature of the spin-wave surface state depends strongly upon the surface exchange and anisotropy. At present, these parameters are not known; nor have they been estimated in any reliable fashion. It is believed that the absence of neighboring spins and/or small distortions at the crystal surface can result in relatively large changes in the superexchange interaction. Low-energy electron-diffraction measurements by Palmberg *et al.*⁸ suggest that the surface exchange in NiO may be considerably smaller than the bulk value.⁹

The theory developed in this paper should be directly applicable to the antiferromagnet RbMnF₃. In this material^{10,11} the Mn²⁺ ions are arranged in a sc two-sublattice antiferromagnetic configuration at temperatures below 82.6°K, the Néel temperature, with lattice

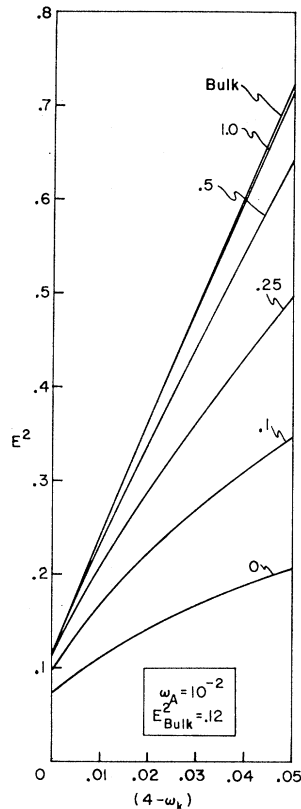


FIG. 5. Dependence of the acoustic surface spin-wave branch on ϵ for $\omega_A = 10^{-2}$ in the long-wave region. The parameter E_{bulk}^2 is the bulk AFMR energy.

⁸ P. W. Palmberg, R. E. De Wames, L. A. Vredevoe, and T. Wolfram, *J. Appl. Phys.* **40**, 1158 (1969).

⁹ R. E. De Wames and T. Wolfram, *Phys. Rev. Letters* **22**, 137 (1969).

¹⁰ C. G. Windsor and R. W. H. Stevenson, *Proc. Phys. Soc. (London)* **87**, 501 (1966).

¹¹ C. G. Windsor, *Proc. Phys. Soc. (London)* **89**, 825 (1966).

spacing 4.24 Å. The ratio of the nearest-neighbor-exchange energy to the anisotropy energy^{12,13} is of the order of 10^{-5} , $\omega_A \approx 3.3 \times 10^{-5}$. Second and more distant neighbor-exchange interactions are negligible.^{10,11}

We have assumed that the external magnetic field lies along the sublattice magnetization, so that our description of the SAFMR mode is only valid¹⁴ below the spin-flop field $(12\omega_A)^{1/2}$. Direct observation of the SAFMR mode for the (100) surface in RbMnF₃ by microwave AFMR does not appear too promising since this mode probably cannot be resolved from the bulk AFMR. On the other hand, since this mode lies so close to the bulk frequency, the excitation amplitude is very weakly damped with depth into the crystal. This implies that a large number of spins participate in the mode. For example, RbMnF₃ has $\omega_A \sim 10^{-5}$, and it is shown in Appendix D that the SAFMR mode has a range on the order of 200 μ . The (111) surface of the simple cube is similar to the (100) surface of the bcc structure in that spins of only one sublattice occurs on the surface. The SAFMR mode for the (111) surface will therefore differ from the bulk mode by a factor of $\sqrt{2}$. The mode is therefore easily resolved from the bulk mode in this case. However, now the surface mode is attenuated rapidly with increasing depth into the crystal, so that the intensity of absorption associated with this surface mode is very small.

APPENDIX A: GREEN'S FUNCTION

In order to construct \bar{G} , the inverse of the matrix \bar{D} defined by Eq. (8), we write

$$\{\bar{G}\}_{nm} = \{\exp[i\hat{\theta}(n+m)] - \exp[i\hat{\theta}|n-m|]\} \hat{C}, \quad (\text{A1})$$

where \hat{C} and $\hat{\theta}$ are 2×2 matrices.

We substitute this form into the matrix equation

$$\bar{D}\bar{G} = \bar{I} \quad (\text{A2})$$

and find that

$$-2 \cos \hat{\theta} = \hat{D}_1^{-1} \hat{D}_0. \quad (\text{A3})$$

The matrix $D_1^{-1} D_0$ may be diagonalized by the similarity transformation, so that

$$\hat{U}^{-1} (\hat{D}_1^{-1} \hat{D}_0) \hat{U} = \begin{pmatrix} -2 \cos \theta_1 & 0 \\ 0 & -2 \cos \theta_2 \end{pmatrix}, \quad (\text{A4})$$

¹² D. T. Teaney, M. J. Freiser, and R. W. H. Stevenson, *Phys. Rev. Letters* **9**, 212 (1962).

¹³ M. J. Freiser, P. E. Seiden, and D. T. Teaney, *Phys. Rev. Letters* **10**, 293 (1963).

¹⁴ For RbMnF₃ it has been suggested that the magnetization can undergo incoherent rotation at fields significantly smaller than the spin-flop field; see P. H. Cole and W. J. Ince, *Phys. Rev.* **150**, 377 (1966). The theory presented here for the SAFMR must also be modified to include the hyperfine anisotropy field due to the polarization of the Mn nuclei. This additional anisotropy field and the effects of nuclear-spin waves become important at liquid-helium temperatures; see, for example, F. Ninio and F. Keffer, *Phys. Rev.* **165**, 735 (1968).

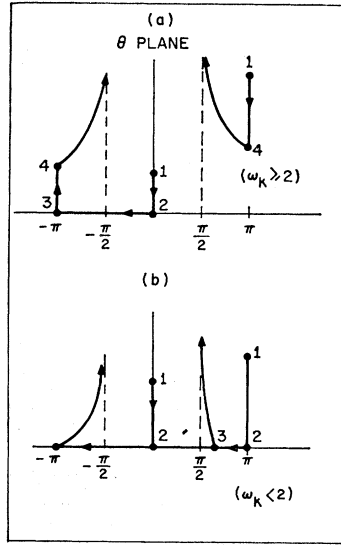


FIG. 6. Contours for the variables θ_1 and θ_2 defined by Eqs. (A6) and (A8). The variable E^2 increases in the direction of the arrows. The values of E^2 corresponding to the labeled points are: (1) $E^2=0$; (2) $E^2=\omega_0^2-(2+\omega_k)^2$ (bottom of bulk continuum); (3) $E^2=\omega_0^2-(\omega_k-2)^2$ or ω_0^2 , whichever is larger (top of bulk continuum); (4) $E^2=\omega_0^2$. (a) For $\omega_k \geq 2$; (b) for $\omega_k \leq 2$.

where

$$U = \begin{pmatrix} (\omega_0 + E)^{1/2} & (\omega_0 + E)^{1/2} \\ (\omega_0 - E)^{1/2} & -(\omega_0 - E)^{1/2} \end{pmatrix} \quad (\text{A5})$$

and

$$-2 \cos \theta_i = \omega_k \pm (\omega_0^2 - E^2)^{1/2}. \quad (\text{A6})$$

In Eq. (A6) the plus sign goes with θ_1 and the minus sign with θ_2 . The boundary condition requires that

$$\hat{C} = (2i \sin \hat{\theta})^{-1} D_1^{-1}.$$

The elements of \bar{G} are most conveniently obtained by calculating them in the representation in which $\hat{\theta}$ is diagonal, and then transforming back to the original representation. In this way we obtain

$$\begin{aligned} \hat{U}[\hat{U}^{-1}\{\bar{G}\}_{nm}D_1\hat{U}]\hat{U}^{-1}D_1^{-1} &= \{\bar{G}\}_{nm} \\ &= U \begin{pmatrix} f_{nm}(\theta_1) & 0 \\ 0 & f_{nm}(\theta_2) \end{pmatrix} U^{-1} D_1^{-1}, \quad (\text{A7}) \end{aligned}$$

where f_{nm} is defined by Eq. (16). When the matrix multiplication indicated by Eq. (A7) is carried out, one obtains the elements of the Green's function given by Eq. (15).

For the semi-infinite crystal, \bar{G} must be finite for arbitrarily large positive integers n and m , so we must require that both θ_1 and θ_2 have positive imaginary parts. We adopt the convention that θ_1 lies in the first quadrant of the upper-half complex plane and θ_2 in the second quadrant of the upper-half complex plane. When

$E^2 > \omega_0^2$, Eq. (A6) takes the form

$$-2 \cos \theta_i = \omega_k \pm i(E^2 - \omega_0^2)^{1/2}. \quad (\text{A8})$$

Typical contours for the θ_1 and θ_2 are sketched in Fig. 6 as a function of E^2 for $\omega_1 > 2$ and $\omega_1 < 2$.

APPENDIX B: VARIABLE x

The determinantal equation for the surface spin-wave spectrum, Eq. (13), is conveniently expressed in terms of the variable x , defined by

$$x = -i \cot \frac{1}{2}(\theta_1 + \theta_2). \quad (\text{B1})$$

In obtaining the cubic equation given by Eq. (19), the boundary condition that θ_1 and θ_2 must have positive imaginary parts is not imposed. In order that a given value of x yield a surface mode, it must be compatible with the definitions of θ_1 and θ_2 . Study of Eq. (A6) reveals that $\text{Re} \frac{1}{2}(\theta_1 + \theta_2)$ is $\frac{1}{2}\pi$ below the bulk continuum and vanishes above the bulk continuum (surface states cannot exist in the bulk continuum). We define x to be x_B below the bulk continuum and x_U above. Then we have

$$\begin{aligned} x_B &= -\tanh \psi \quad (\text{below bulk continuum}), \\ x_U &= -\coth \psi \quad (\text{above bulk continuum}), \\ \psi &= \text{Im} \frac{1}{2}(\theta_1 + \theta_2), \end{aligned} \quad (\text{B2})$$

The physically acceptable solutions of the cubic equation therefore have x negative.

We find that

$$x_B(E, \omega_k) = \frac{\{[\frac{1}{2}(E' + \omega_k)]^2 - 1\}^{1/2} + \{[\frac{1}{2}(E' - \omega_k)]^2 - 1\}^{1/2}}{-E'}, \quad (\text{B3})$$

where

$$E' = (\omega_0^2 - E^2)^{1/2}. \quad (\text{B4})$$

For x_U we find

$$x_U(E, \omega_k) = -\left(\{[\frac{1}{2}(E' + \omega_k)]^2 - 1\}^{1/2} - \{[\frac{1}{2}(E' - \omega_k)]^2 - 1\}^{1/2}\right)(E')^{-1}, \quad (\text{B5})$$

for $\omega_k \geq 2$ and with $\omega_0^2 - (\omega_k - 2)^2 \leq E^2 \leq \omega_0^2$.

If $\omega_k \leq 2$ then the upper band edge of the continuum occurs at ω_0^2 , and for $E^2 > \omega_0^2$ we find

$$x_U(E, \omega_k) = -\left\{\frac{1}{2}\Lambda_k + \frac{1}{2}[\Lambda_k^2 + 4(\omega_k/\mathcal{E})^2]^{1/2}\right\}^{1/2}, \quad (\text{B6})$$

with

$$\Lambda_k = 1 - (\omega_k/\mathcal{E})^2 + (2/\mathcal{E})^2, \quad \mathcal{E} = (E^2 - \omega_0^2)^{1/2}. \quad (\text{B7})$$

The above equations for x_B and x_U may be used to determine whether or not a given root of the cubic equation, Eq. (19), corresponds to a physically acceptable solution.]

APPENDIX C: CALCULATION OF ϵ_b

In Sec. IV A it was pointed out that, for $\omega_A = \Delta\omega_A = 0$, $x = -\sqrt{2}/3$, $E=0$ is a solution of the cubic equation in-

dependent of ϵ when $\omega_k \equiv 4$. In order to determine the value of ϵ above which the acoustic surface branches are truncated near $k=0$, it is necessary to inspect the behavior of the $-\sqrt{\frac{2}{3}}$ root in the limit as $k \rightarrow 0$ (or $\omega_k \rightarrow 4$) rather than at $k \equiv 0$. If we take $\omega_k = 4 - \alpha$, then the region below the bottom of the continuum extends from $E=0$ to $E^2 = 36 - (6 - \alpha)^2 = E_B^2$. Calculation of x from Eq. (B3) shows that, for small α , x varies from $-\sqrt{\frac{2}{3}} - \frac{1}{6}\sqrt{\alpha}$ at $E=0$ to $-\sqrt{\frac{2}{3}} + (\sqrt{\frac{2}{3}})(\alpha/24)$ at $E=E_B$. If we write as a solution of the cubic equation $x = -\sqrt{\frac{2}{3}} + \beta$, then we find by perturbation theory that

$$\beta = \frac{\alpha \left[\left(\sqrt{\frac{2}{3}} - \frac{2}{3} \right) (1 - \epsilon)^2 - \frac{1}{3} (1 - \epsilon) \right]}{1 + (4 - 6\sqrt{\frac{2}{3}})(1 - \epsilon)}.$$

For $\epsilon > 1$, β is positive and we find the critical value of ϵ by requiring that β be greater than the corresponding shift in the value of x as calculated from Eq. (B3):

$$\beta \geq (\alpha/24) \left(\frac{2}{3} \right)^{1/2}. \quad (C1)$$

When Eq. (C1) holds, the value of x calculated from the cubic equation does not correspond to a physical solution. Solution of Eq. (C1) (for $\epsilon > 1$) leads to the value 1.107 for ϵ_b .

APPENDIX D: EIGENVECTORS

From the relation

$$(\bar{I} + \bar{G}\Delta\bar{D})U = 0 \quad (D1)$$

we obtain, for $u_1^{(a)}$ normalized to unity, the amplitude of excitation $u_n^{(\mu)}$ for the surface eigenmodes. For the surface, we find that

$$u_1^{(a)} = 1, \quad u_1^{(b)} = \frac{-[1 + \{\bar{G}\}_{11}^{11}\Delta\omega_0 - \{\bar{G}\}_{11}^{12}\Delta\omega_k]}{\{\bar{G}\}_{11}^{11}\Delta\omega_k - \{\bar{G}\}_{11}^{12}\Delta\omega_0}, \quad (D2)$$

and for $n > 1$, we find

$$u_n^{(a)} = -[\{\bar{G}\}_{n1}^{11}\Delta\omega_0 - \{\bar{G}\}_{n1}^{22}\Delta\omega_k] - [\{\bar{G}\}_{n1}^{11}\Delta\omega_k - \{\bar{G}\}_{n1}^{12}\Delta\omega_0]u_1^{(b)}, \quad (D3)$$

$$u_n^{(b)} = -[\{\bar{G}\}_{n1}^{21}\Delta\omega_0 - \{\bar{G}\}_{n1}^{22}\Delta\omega_k] - [\{\bar{G}\}_{n1}^{21}\Delta\omega_k - \{\bar{G}\}_{n1}^{22}\Delta\omega_0]u_1^{(b)}.$$

The Green's-function matrix elements are defined by Eq. (15); in Eqs. (D2) and (D3) the matrix elements are

evaluated at the energy of the surface eigenmode. We consider here the behavior of the $k=0$ surface mode for $\epsilon=1$, which lies very near to the bulk AFMR energy. According to Eq. (26), this surface state has energy

$$E_0^2 = 12\omega_A + \frac{1}{2}\omega_A^2, \quad (D4)$$

while the bulk energy is $12\omega_A + \omega_A^2$. Since the surface mode lies below the bulk, θ_1 and θ_2 have the form

$$\theta_1 = \pi + i\psi_1, \quad \theta_2 = i\psi_2. \quad (D5)$$

The excitation amplitudes for this SAFMR mode are

$$u_1^{(a)} = 1, \quad u_1^{(b)} = \frac{-\{1 - \frac{1}{2}[(\omega_0 + E_0)/(\omega_0 - E_0)]^{1/2} (e^{-\psi_1} + e^{-\psi_2})\}}{\frac{1}{2}(-e^{-\psi_1} + e^{-\psi_2})},$$

$$u_n^{(a)} = -\frac{1}{2}[(\omega_0 + E_0)/(\omega_0 - E_0)]^{1/2} [(-1)^n e^{-n\psi_1} - e^{-n\psi_2}] - \frac{1}{2} [(-1)^n e^{-n\psi_1} + e^{-n\psi_2}] u_1^{(b)}, \quad (D6)$$

$$u_n^{(b)} = -\frac{1}{2} [(-1)^n e^{-n\psi_1} + e^{-n\psi_2}] - \frac{1}{2} [(\omega_0 - E_0)/(\omega_0 + E_0)]^{1/2} \times [(-1)^n e^{-n\psi_1} - e^{-n\psi_2}] u_1^{(b)},$$

where

$$\cosh\psi_1 = 2 + \frac{1}{2}(\omega_0^2 - E_0^2)^{1/2}, \quad \cosh\psi_2 = \frac{1}{2}(\omega_0^2 - E_0^2)^{1/2} - 2. \quad (D7)$$

For large n , terms in $e^{-n\psi_2}$ dominate and we find, making use of Eq. (D7), that

$$u_n^{(a)} \rightarrow -u_n^{(b)} \rightarrow \exp(-n\omega_A/\sqrt{24}). \quad (D8)$$

This surface mode is long-range for small ω_A . For example, for $\omega_A \sim 10^{-5}$ the surface wave according to Eq. (D8) decays to e^{-1} of its surface value in about 5×10^5 atomic layers or about 200 μ . For a 1-mm-thick sample the intensity of absorption of this mode would be on the order of 40% of the bulk AFMR intensity.

The difference between the bulk and surface mode energies is very small:

$$\frac{1}{2}\omega_A^2 / (12\omega_A)^{1/2} \approx 5 \times 10^{-9}. \quad (D9)$$

Thus it is doubtful that the two absorption lines could be resolved.